RESEARCH ARTICLE

Functional Ecology — BRITISH ECOLOGICAL SOCIETY

Coordination of hydraulic and morphological traits across dominant grasses in eastern Australia

Robert J. Griffin-Nolan[1,2,3] | Jeff Chieppa[1,4] | Alan K. Knapp[5] | Uffe N. Nielsen[1] | David T. Tissue[1]

[1]Hawkesbury Institute for the Environment, Western Sydney University, Richmond, New South Wales, Australia

[2]Department of Biology, Santa Clara University, Santa Clara, California, USA

[3]Department of Biological Sciences, California State University, Chico, California, USA

[4]Department of Biological Sciences, Texas Tech University, Lubbock, Texas, USA

[5]Department of Biology and Graduate Degree Program in Ecology, Colorado State University, Fort Collins, Colorado, USA

Correspondence
Robert J. Griffin-Nolan
Email: rgriffinnolan@scu.edu

Abstract

1. Leaf hydraulic traits characterize plant drought tolerance and responses to climate change. Yet, plant hydraulics are biased towards northern hemisphere woody species. We collected rhizomes of several perennial grass species along a precipitation gradient in eastern Australia and grew them in an experimental pot study to investigate potential trade-offs between drought tolerance and plant morphology.

2. We measured the following leaf hydraulic traits: the leaf water potential (Ψ_{leaf}) at 50% and 88% loss of leaf hydraulic conductance ($P50_{Kleaf}$ and $P88_{Kleaf}$), the Ψ_{leaf} at 50% loss of stomatal conductance ($P50_{gs}$), leaf turgor loss point (TLP), leaf dry matter content (LDMC), leaf modulus of elasticity (ε), and the slope of the relationship between predawn and midday Ψ_{leaf}. We also measured basal area, tiller density, seed head density, root collar diameter, plant height, and aboveground biomass of each individual.

3. As expected, grass species varied widely in leaf-level drought tolerance, with loss of 88% hydraulic conductance occurring at a Ψ_{leaf} ranging from −1.52 to −4.01 MPa. However, all but one species lost leaf turgor, and most reached $P50_{gs}$ before this critical threshold. Taller more productive grass species tended to have drought vulnerable leaves characterized by low LDMC and less negative $P88_{Kleaf}$. Species with greater tiller production experienced stomatal closure and lost turgor at more negative Ψ_{leaf}. Although our sample size was limited, we found no relationships between these species' traits and their climate of origin.

4. Overall, we identified important hydraulic and morphological trade-offs in Australian grasses that were surprisingly similar to those observed for woody plants: (1) xylem of taller species was less drought tolerant and (2) turgor loss occurs and stomatal closure begins before significant loss of K_{leaf}. These data build upon a small yet growing field of grass hydraulics and may be informative of species responses to further drought intensification in Australia.

KEYWORDS
grass, leaf hydraulics, plant traits, stomatal conductance, turgor loss point

1 | INTRODUCTION

Plant traits describe the resource use strategies of species and individuals along the "fast-slow plant economic spectrum" ranging from the acquisitive (fast) to the conservative (slow) strategy (Díaz et al., 2016; Reich, 2014). Increasingly, plant traits are being used to model species distributions (Benito Garzón et al., 2019), quantify functional diversity (Laliberté & Legendre, 2010), and improve our understanding of ecosystem functioning (Funk et al., 2017; Griffin-Nolan, Blumenthal, et al., 2019; Suding et al., 2008; but see van der Plas et al., 2020). Given the expansive list of plant traits that can potentially be measured (Perez-Harguindeguy et al., 2016), identifying the appropriate traits to measure for a given environmental and/or ecological context is critical for testing hypotheses in plant functional ecology (Rosado et al., 2013). For example, hydraulic traits (e.g. physiological traits involved in plant water status, transport, and storage) are important for understanding plant, community, and ecosystem responses to shifting precipitation regimes that are occurring due to climate change (Brodribb et al., 2020; Griffin-Nolan et al., 2018). Although hydraulic traits are predominantly measured on woody species with a high capacity for water storage (Griffin-Nolan et al., 2018), the field of non-woody plant hydraulics is rapidly expanding (Griffin-Nolan, Ocheltree, et al., 2019; Holloway-Phillips & Brodribb, 2011; Jacob et al., 2022; Jardine et al., 2021; Lens et al., 2016; Májeková et al., 2021; Ocheltree et al., 2016; Sonawane et al., 2021; Wilcox et al., 2021; Zhou et al., 2020).

The capacity to move water safely and efficiently is a primary determinant of plant drought tolerance and survival. During severe drought, xylem cavitation can occur when air bubbles form and spread throughout xylem under extreme negative pressure, thereby blocking the flow of water through plants (Zimmermann, 1983). Variation in leaf hydraulic conductance (K_{leaf}; flow rate/water potential driving force) is in part regulated by stomatal conductance (g_s) (Brodribb & Holbrook, 2003) among other anatomical determinants (e.g. vein density and diameter; Blackman et al., 2010; Brodribb et al., 2016; Sack et al., 2003; Scoffoni et al., 2011). Conservative species operate in a safer hydraulic margin either by closing stomata earlier as soil moisture declines, thereby avoiding declines in leaf xylem water potential (Ψ_{leaf}), or by increasing xylem resistance to cavitation. Acquisitive species, on the other hand, operate under narrower safety margins, which allows them to be more productive at the expense of greater risk of hydraulic failure (Tardieu & Simonneau, 1998). Rarely are plant drought strategies characterized simply as either acquisitive or conservative, as it is a spectrum involving the complex coordination of multiple physiological responses to dehydration (Bartlett et al., 2016). Understanding how such strategies vary among species and across environmental gradients may improve our predictions of species distributions and ecosystem responses to increased aridity with climate change (Konings & Gentine, 2017; Martínez-Vilalta et al., 2014; McDowell et al., 2008; Skelton et al., 2015).

The degree of stomatal regulation over leaf water status can be quantified as the difference between critical Ψ_{leaf} thresholds corresponding to significant declines in g_s and K_{leaf} (Skelton et al., 2015), whereby conservative species close stomata before significant loss of K_{leaf} occurs. The point of stomatal closure can also be inferred from leaf turgor loss point (TLP)—the Ψ_{leaf} at which cells lose turgor and leaves begin to wilt—a trait that is considered a proxy for stomatal closure (Meinzer et al., 2016; but see Farrell et al., 2017). Alternatively, plant regulation of Ψ_{leaf} can be interpreted from the slope of the linear relationship between pre-dawn and midday Ψ_{leaf} (Martínez-Vilalta et al., 2014), although this is not necessarily associated with stomatal sensitivity (Martínez-Vilalta & Garcia-Forner, 2017). Assuming pre-dawn Ψ_{leaf} is representative of soil moisture conditions (Ritchie & Hinckley, 1975; but see Donovan et al., 2001), the slope for highly conservative species would be close to zero, indicative of little change in midday Ψ_{leaf} as soil moisture declines, whereas the slope of the relationship for more acquisitive species would be closer to one as Ψ_{leaf} tracks soil moisture. The indirect method of Martínez-Vilalta et al. (2014) is particularly useful for ecosystem-scale measurements of plant water use strategies as leaf water potential can be estimated from remote sensing (Konings & Gentine, 2017).

Herbaceous plants are vulnerable to declines in K_{leaf} (Lens et al., 2016) yet receive relatively less attention than woody species (Griffin-Nolan et al., 2018). The adaptive significance of xylem resistance to cavitation is likely different for short-statured herbaceous plants compared to woody species. Specifically, tall woody plants must maintain hydraulic conductance of the same tissue for multiple growing seasons, while many perennial herbs can withstand significant loss of K_{leaf} and aboveground tissue during drought and re-sprout from belowground buds following extreme drought events (Vander Weide et al., 2014). Indeed, the xylem water potential at 50% loss of leaf hydraulic conductance (P50) was uncoupled from drought survival of several perennial grass species (Ocheltree et al., 2016). However, there is evidence that hydraulic traits are important determinants of herbaceous plant drought strategies and species distributions. For example, leaf TLP of graminoids was positively associated with mean annual precipitation (MAP) in the Great Plains, where more drought tolerant species with more negative TLP inhabited drier regions (Griffin-Nolan, Ocheltree, et al., 2019). Additionally, herbaceous species sensitivity to inter-annual variability in precipitation (assessed as % change in relative cover per mm change in precipitation) in this same region was associated with leaf osmotic potential at full turgor—the primary determinant of TLP (Bartlett et al., 2012)—as well as leaf dry matter content (LDMC), suggesting slow-growing drought resistant grasses and forbs will be favoured during drought years and in a chronically drier climate (Wilcox et al., 2021). Importantly, both LDMC and osmotic potential are strongly correlated with P50 across grass species (Griffin-Nolan, Ocheltree, et al., 2019), suggesting climate may also drive broad patterns of K_{leaf} for grasses as well as species rankings from conservative to acquisitive strategies. Thus, while no direct link between grass survival and hydraulic traits was observed in greenhouse conditions (Ocheltree et al., 2016), the hydraulic trait-performance

relationships that have been observed in the field for grasses warrant further investigation.

Hydraulic traits can vary widely within and between species (Anderegg, 2015), which is helpful for distinguishing drought tolerant from intolerant species/populations. However, species may converge on similar hydraulic trait values yet respond differently to drought and other environmental perturbations due to differences in morphology (Hoover et al., 2019). Indeed, the second axis of global variation in plant form and function (in addition to the fast-slow spectrum) is one that describes plant size and morphology (Díaz et al., 2016; Sandel et al., 2016). It is therefore important to identify whether and how different morphological trait syndromes are coordinated with hydraulic traits. This is not only important for understanding ecosystem functions such as net primary productivity but also ecosystem susceptibility to fire, a common disturbance in grasslands and savannahs. For many grass species, the majority of aboveground biomass is composed of photosynthetic tissue (e.g. leaf and sheath). The desiccation of leaf material could lead to dehydration of the entire above-ground portion of the plant. Given that foliage moisture content and total biomass are linked to fire intensity and its rate of spread (Simpson et al., 2022), the linkages between drought tolerance and plant size could massively impact ecosystem fire dynamics.

In this study, we quantified seven leaf hydraulic traits of seven perennial grass species commonly found in eastern Australian rangelands. Much of eastern Australia is both drought- and fire-prone and expected to become drier with climate change (De Kauwe et al., 2020; Delworth & Zeng, 2014; Timbal & Fawcett, 2013). Additionally, interannual variability in precipitation is relatively high in this region compared to elsewhere (Van Etten, 2009). We collected ecotypes of these grass species across sites varying in MAP and inter-annual variation in precipitation (i.e. the coefficient of variation [CV] of MAP) and measured both hydraulic and stomatal sensitivity to dehydration as well as traits linked to herbaceous plant drought tolerance (e.g. TLP and LDMC) and morphology. Our primary goal was to assess whether hydraulic and morphological traits were coordinated and associated with species climate affiliations. We tested the hypotheses that (i) hydraulic traits are coordinated across the conservative-acquisitive spectrum (Reich, 2014), (ii) hydraulic traits are associated with aboveground biomass and plant size (McGregor et al., 2021) and (iii) hydraulic traits predict species climate affiliations (Griffin-Nolan, Ocheltree, et al., 2019).

2 | MATERIALS AND METHODS

2.1 | Plant collection and propagation

We collected a total of seven grass species from four sites in eastern Australian rangelands varying in MAP and CV of MAP (n = 11 Ecotypes; Table 1; Figure S1). Samples were taken with permission

TABLE 1 Climate characteristics for each collection site.

Site	Species	Code	GPS coordinates	MAP (mm)	MAP CV (%)	AI
Broken Hill, NSW	*Astrebla pectinate* (Barley Mitchell grass)	BH ASPE	−32.1145108, 141.8027844	251	28%	6.1
	Austrostipa scabra (Rough spear-grass)	BH AUSC	−32.1145108, 141.8027844	251	28%	6.1
Tibooburra, NSW	*Astrebla pectinate* (Barley Mitchell grass)	TI ASPE	−29.607821, 141.710996	265	52%	8.9
	Aristida contorta (Kerosene grass)	TI ARCO	−29.607821, 141.710996	265	52%	8.9
Charleville, QLD	*Astrebla lappacea* (Curly Mitchell grass)	CH ASLA	−26.3666688, 146.1422040	442	53%	3.9
	Aristida contorta (Kerosene grass)	CH ARCO	−26.3666688, 146.1422040	442	53%	3.9
	Cenchrus ciliaris (Buffel grass)	CH CECI	−26.3666688, 146.1422040	442	53%	3.9
	Themeda triandra (Kangaroo grass)	CH THTR	−26.3666688, 146.1422040	442	53%	3.9
Nyngan, NSW	*Austrostipa scabra* (Rough spear-grass)	NY AUSC	−31.643647, 146.646653	446	31%	3.17
	Cenchrus ciliaris (Buffel grass)	NY CECI	−31.5607735, 146.6140118	446	31%	3.17
	Chloris truncate (Windmill grass)	NY CHTR	−31.133180, 147.506959	446	31%	3.17

Note: Precipitation data from the Bureau of Meteorology (http://bom.gov.au), averaged from 2002–2012. MAP = mean annual precipitation; MAP CV = Coefficient of variation of MAP; AI = aridity index. The aridity index was calculated as the ratio of mean annual potential evapotranspiration and mean annual precipitation (i.e. higher values equal greater aridity; Deveautour et al., 2020). All species are C_4 grasses except *Austrostipa scabra*, which is C_3.

from private land owners. Species included *Cenchrus ciliaris* (Buffel grass, C_4), *Austrostipa scabra* (Rough spear-grass, C_3), *Chloris truncate* (Windmill grass, C_4), *Astrebla pectinate* (Barley Mitchell grass, C_4), *Aristida contorta* (Kerosene grass, C_4), *Astrebla lappacea* (Curly Mitchell grass, C_4), and *Themeda triandra* (Kangaroo grass, C_4). Not all species were present at each site. We selected sites to represent high and low interannual rainfall variability across a moderate rainfall gradient (251 to 446 mm MAP). We selected these target species based on their high abundance at collection sites on previous trips (Chieppa, Power, et al., 2020) and their general distributions, which spanned the region (Cunningham & Leigh, 2011). At each site, we unearthed rhizomes ($n = 12$) of selected species and stored them on ice in plastic bags with a moist paper towel to prevent desiccation. We pruned the roots and tillers so that the crown consisted of 50% above- and 50% below-ground components; each section was 10 cm in length. Samples were transported to Richmond, New South Wales (NSW), where we planted rhizomes in 7.5-litre pots filled with moderately fertile sandy loam soil collected from Menangle, NSW. Soil characteristics were as follows: pH 4.4, 0.01 M $CaCl_2$, total organic carbon 1.21%, total N 520 mg kg^{-1} and total P 230 mg kg^{-1} (Zhang et al., 2018). Plants were initially propagated on a steel-mesh table in an enclosed polytunnel that reduced ambient light by ca. 25%. We installed irrigation rings in each pot to maintain saturated soil moisture during the initial establishment period (December 22, 2016 through February 2, 2017) and monitored the height and number of leaves of each individual.

Once plants had reached a minimum of five tillers, each with >3 leaves, we moved the pots to an outdoor open-sided polytunnel (48 m long by 9 m wide, maximum height of 4.6 m), where they grew under natural light, photoperiod and temperature conditions of an eastern NSW summer (Figure S1). Roofs were made of 180-micron plastic (Argosee, Australia) to intercept all ambient precipitation but minimize light interception. To avoid root growth into the soil, we placed plots on pallets. We subjected plants to a "priming drought" by removing irrigation rings for 2 weeks before hand-watering back to saturation to mimic regular soil drying and re-wetting cycles that these species experience in the field. Pots were maintained at saturated soil moisture conditions by watering every day for an additional 2 weeks before measuring physiological traits.

2.2 | Pressure-volume curves

To determine pressure-volume (p-v) curve parameters, we collected one tiller from six randomly selected pots per ecotype and placed it in a vial of water in a dark room overnight to allow full tissue rehydration. We then used the bench drying method (Schulte & Hinckley, 1985) to determine p-v curve parameters. Briefly, we wrapped a recently expanded mature leaf from each tiller in parafilm wax and cut it near the leaf base (parafilm was weighed and subtracted from subsequent leaf weight measurements). Immediately after cutting, we placed the leaf in a Scholander-style pressure chamber (PMS Instruments) to measure Ψ_{leaf}. Following water potential determination, the leaf and parafilm

were weighed on a micro-balance (± 0.1 mg). We then sealed the leaf in a plastic bag and placed it in a dark drawer to allow slow dehydration. We repeated this process approximately 10 times for each leaf or until Ψ_{leaf} reached -4 MPa. At this point, the leaf was rehydrated, scanned for leaf area at 300 dpi, dried for 48 h at 60°C and weighed. We estimated leaf area using ImageJ software (https://imagej.nih.gov/ij/) and determined leaf turgor loss point (TLP), capacitance (C_{Leaf}) and modulus of elasticity (ε) following standard protocols (Koide et al., 1989; Turner, 1988); data were averaged across pots for each ecotype. Finally, we estimated leaf dry matter content (LDMC) as leaf dry mass/fully hydrated leaf mass.

2.3 | Leaf vulnerability curves

We measured declines in g_s and K_{leaf} in situ on a subset of plants during an extended drought experiment, with the length of dry-down depending on the species-specific rate of decline in g_s and K_{leaf}. Specifically, following recovery from the initial "priming drought", we stopped irrigating pots and tracked diurnal trends in both midday and pre-dawn Ψ_{leaf} for approx 4–6 weeks, depending on the species. To reduce the time from leaf clipping to Ψ_{leaf} measurements, we restricted our sampling to 16 pots per day with at least 2 pots/ecotype measured each day. For each measurement, we selected a single tiller with at least 3 leaves. Before sunrise, we cut the basal leaf of each tiller and estimated pre-dawn Ψ_{leaf} using a Scholander style pressure chamber. Prior to midday measurements (i.e. between 9:30 and 11:30 h.), we estimated g_s on the apical fully expanded leaf using an SC-1 steady state leaf porometer (Decagon Devices), which was calibrated prior to each measurement. We then cut this same leaf to estimate midday Ψ_{leaf}. Leaves were sealed in plastic bags with a moist paper towel for at least 3 min prior to measurement of Ψ_{leaf} to ensure equilibration of any gradient in Ψ_{leaf} across the leaf.

Immediately following midday Ψ_{leaf} sampling, we estimated K_{leaf} of the remaining leaf of each tiller using the rehydration kinetics method (Brodribb & Holbrook, 2003). Previous studies on grass hydraulics have measured K_{leaf} at this time to capture midday leaf function (Ocheltree et al., 2016). We removed this leaf with a razor while the leaf was submerged in filtered de-ionized water. We kept the leaf submerged for a pre-determined rehydration time (5–120 s depending on pre-dawn Ψ_{leaf}) before cutting the leaf slightly above the water line and placing it in a pressure chamber to determine final rehydrated leaf water potential (Ψ_f). Using the midday Ψ_{leaf} measurement as our initial leaf water potential (Ψ_o), we calculated K_{leaf} as follows:

$$K_{leaf} = \frac{C_{leaf} \times \ln\left(\frac{\Psi_o}{\Psi_f}\right)}{t},$$

where t is the rehydration time in seconds and C_{leaf} is mean leaf capacitance quantified from p-v curves ($n = 6$). We calculated K_{leaf} in this way for ~20 leaves per ecotype and filled in any gaps in the vulnerability curve using bench-dried tillers (~30 total measurements per ecotype).

We estimated maximum K_{leaf} as the average of 3–5 values between Ψ_o of -0.5 and -1 MPa. Using the FITPLC package in R Statistical

Programming (Duursma & Choat, 2017), we fit Weibull functions to a plot of K_{leaf} and Ψ_o for each ecotype to determine the Ψ_{leaf} at 50% and 88% loss of hydraulic conductance (P50$_{kleaf}$ and P88$_{kleaf}$, respectively; Figure 1). The same approach was used to estimate Ψ_{leaf} at 50% loss of stomatal conductance (P50$_{gs}$) from the relationship between midday Ψ_{leaf} and g_s (Figure 2). For most species, we did not record a zero value of g_s (P100$_{gs}$) and did not want to extrapolate beyond our measured values. Therefore, P50$_{gs}$ reflects partial stomatal closure.

2.4 | Morphological traits

For the subset of pots that were used for hydraulic trait measurements, we measured plant morphological traits approximately

17 weeks after propagation (late April). Ontogenetically, these measurements reflect the morphology of fully mature individuals at the end of an Australian growing season. Specifically, we measured tiller density and counted the number of seed heads in each pot. We also estimated maximum height (mm), basal area (BA; mm^2) and root collar diameter (RCD, mm). Finally, we clipped all aboveground biomass, which was oven-dried (>48 h at 60°C) and weighed.

2.5 | Data analysis

We estimated the degree of regulation over leaf hydration status as the slope of the linear relationship between pre-dawn and midday leaf Ψ_{leaf} (Martínez-Vilalta et al., 2014). Specifically, we ran a linear mixed effects model including random slopes and intercepts for
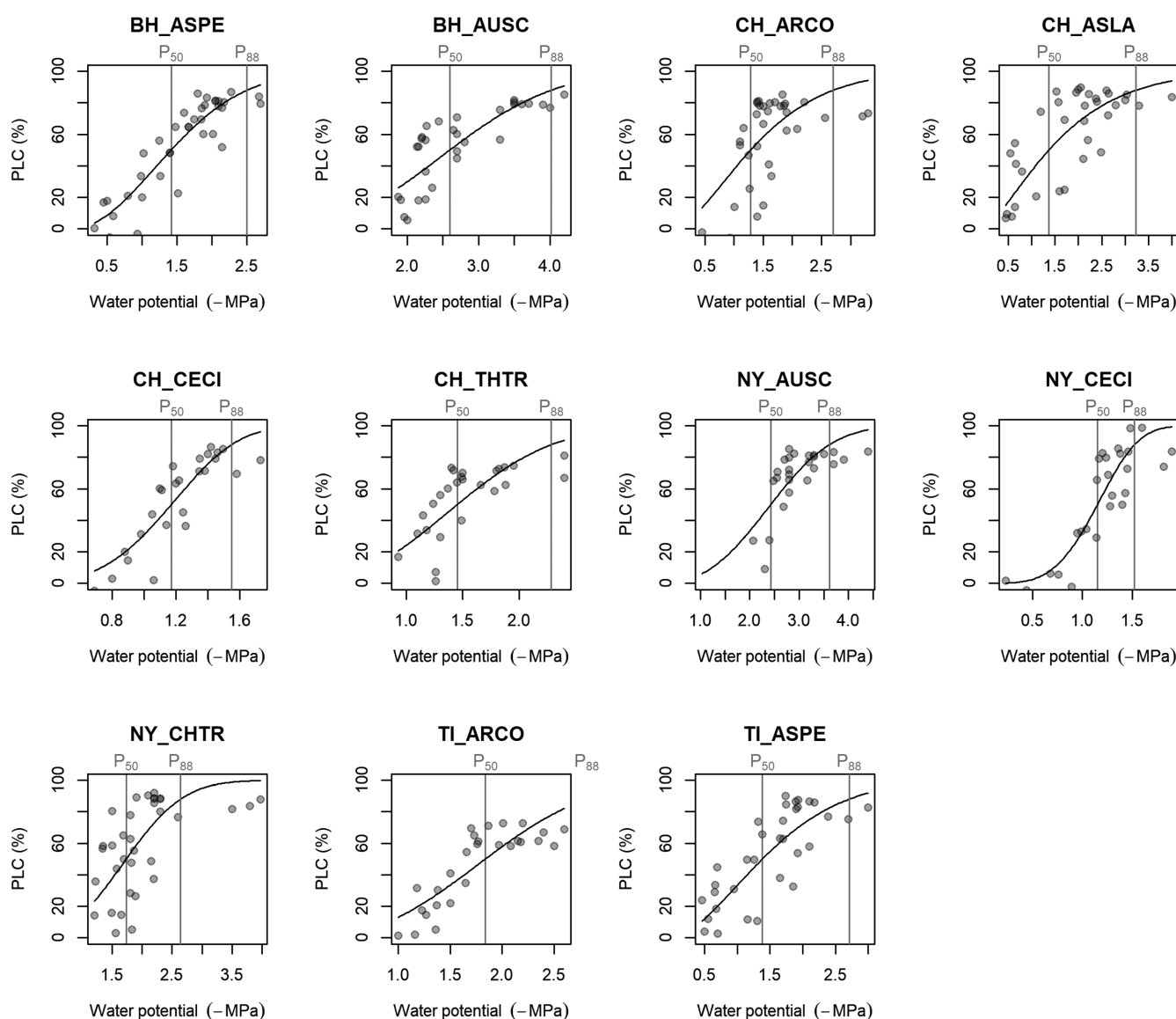
FIGURE 1 Leaf hydraulic vulnerability curves for each ecotype shown as percent loss of hydraulic conductance (K_{leaf}). Fitted models represent Weibull functions and the two vertical lines denote P50$_{kleaf}$ and P88$_{kleaf}$, or the leaf water potential at 50% and 88% loss of conductance, respectively. See Table 1 in the main text for species and site abbreviations.
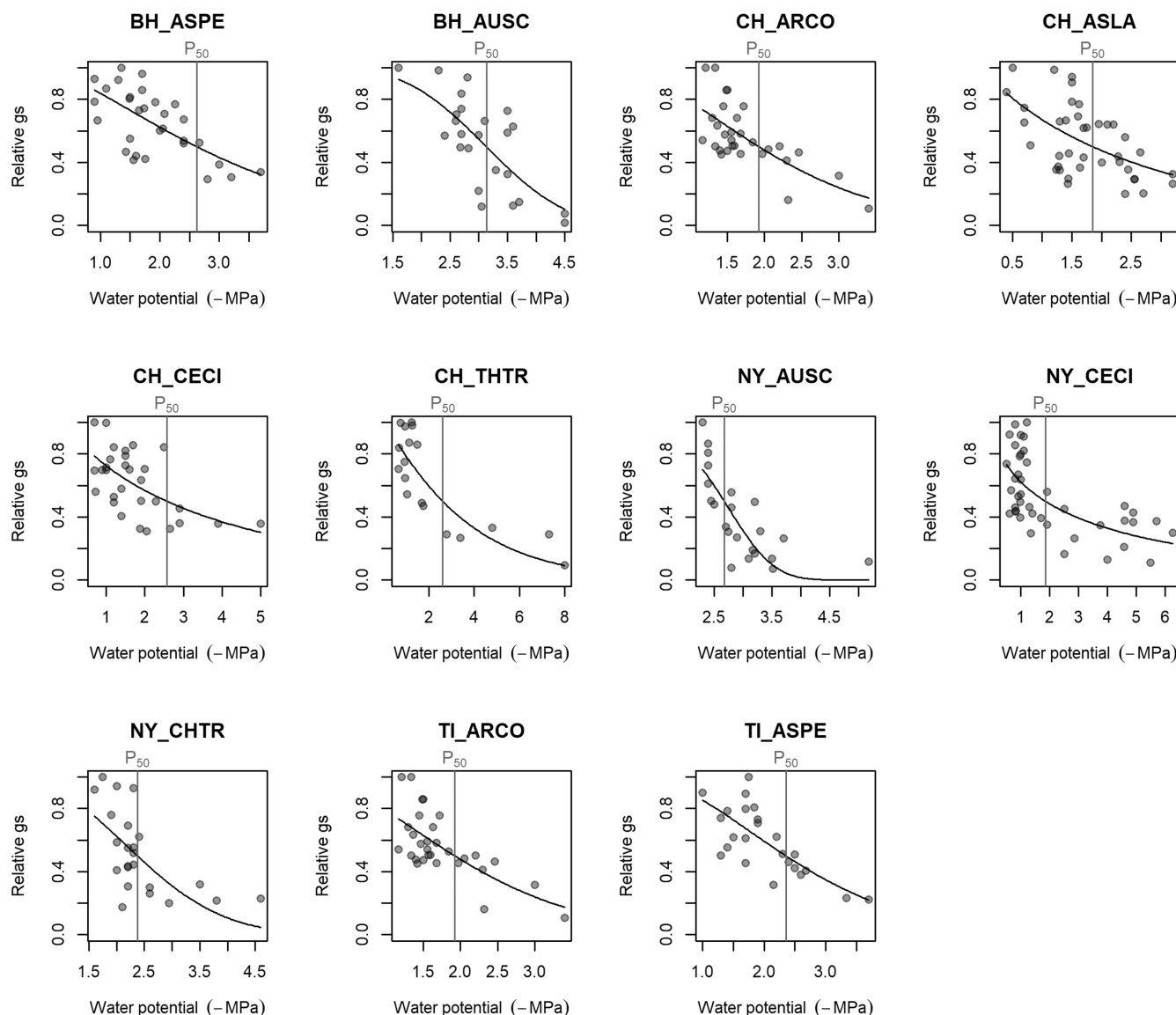
FIGURE 2 Stomatal dehydration curves for each ecotype. Stomatal conductance (g_s) is shown in units relative to maximum g_s. Fitted models represent Weibull functions and the vertical line denotes P50$_{gs}$, or the leaf water potential at 50% stomatal closure. See Table 1 in main text for species and site abbreviations.

each ecotype and a random effect of pot (i.e. individual). According to this method, a slope of one suggests loose regulation of leaf water status (midday Ψ_{leaf}) as soil water potential (pre-dawn Ψ_{leaf}) declines. In contrast, a slope closer to zero would reflect a conservative water-use strategy with tight regulation of Ψ_{leaf}.

We assessed the coordination of hydraulic and morphological traits across ecotypes with Pearson's *r* correlation using the *cor* function in R. For this analysis, LDMC was grouped with hydraulic traits as it is estimated from p-v curves and is a common metric of drought tolerance. We scaled and centered all traits prior to analysis for ease of visualization. We included all scaled and centered trait data (both morphological and hydraulic) in a principal component analysis (PCA) to explore different axes of trait variation. The PCA was run using the *prcomp* function in R. Finally, we tested whether climate of origin was associated with species positions along these axes by extracting individual scores along each axis and including

those values as response variables in a multivariate multiple regression with MAP, the CV of MAP, and AI as predictor variables. We used R version 4.2.2 for all analyses and data visualization.

3 | RESULTS

Species varied in their sensitivities of K_{leaf} to dehydration with P50$_{Kleaf}$ ranging from −1.15 to −2.6 MPa, and P88$_{Kleaf}$ ranging from −1.52 to −4.01 MPa (Figure 1, Table 2). The Ψ_{leaf} at 50% stomatal closure (P50$_{gs}$) ranged from −1.85 to −3.1 MPa (Figure 2, Table 2). All 11 ecotypes experienced 50% loss of K_{leaf} prior to P50$_{gs}$ (Figure 3a). Seven of 11 ecotypes reached P50$_{gs}$ (Figure 3b) and all but one ecotype (NY CECI) lost leaf turgor prior to experiencing 88% loss of K_{leaf} (Figure 3d). Across all species, the slope of the linear relationship between pre-dawn and midday Ψ_{leaf} was 0.76 (Figure 4),

TABLE 2 Hydraulic and morphological traits measured for each ecotype. Shown are trait means with standard error (or 95% CI in the case of hydraulic traits) in parentheses when available. For $P88_{kleaf}$, the 95% confidence interval was constrained by the limit of the data collection range, and so NA is shown when the interval for the curve cannot be predicted beyond the data. For slope, the value in brackets represents the species ranking from strong [1] to weak [11] regulation of plant water status. $P50_{kleaf}$ = leaf water potential at 50% loss of leaf hydraulic conductance (MPa); $P88_{kleaf}$ = leaf water potential at 88% loss of leaf hydraulic conductance (MPa); $P50_{gs}$ = leaf water potential at 50% of maximum stomatal conductance (MPa); TLP = leaf turgor loss point (MPa); ε = leaf modulus of elasticity (MPa); LDMC = leaf dry matter content (LDMC); Slope = the slope coefficient for the relationship between pre-dawn and midday Ψ_{leaf}. RDC = root collar diameter. See Table 1 for ecotype abbreviations.

Ecotype	BH ASPE	BH AUSC	TI ASPE	TI ARCO	CH ASLA
$P50_{kleaf}$	−1.42 (−1.54, −1.29)	−2.60 (−2.76, −2.39)	−1.38 (−1.61, −1.17)	−1.84 (−1.97, −1.7)	−1.37 (−1.69, −1.07)
$P88_{kleaf}$	−2.51 (NA, −2.25)	−4.01 (NA, −3.65)	−2.71 (NA, −2.13)	−2.81 (NA, −2.38)	−3.23 (NA, −2.56)
$P50_{gs}$	−2.62 (−3.26, −2.36)	−3.13 (−3.44, −2.88)	−2.35 (−2.57, −2.12)	−1.92 (−2.11, −1.73)	−1.85 (−2.20, −1.47)
TLP	−1.93 (−2.06, −1.80)	−2.59 (−2.91, −2.27)	−1.97 (−2.18, −1.75)	−1.19 (−1.45, −0.93)	−2.01 (−2.58, −1.45)
ε	15.04 (3.31)	16.61 (2.37)	15.59 (2.98)	11.42 (2.66)	11.78 (1.29)
LDMC	0.35 (0.009)	0.33 (0.02)	0.39 (0.07)	0.28 (0.01)	0.33 (0.03)
Slope	0.62 [2]	0.37 [1]	0.744 [4]	0.98 [11]	0.76 [5]
Aboveground Biomass (g)	8.62 (1.47)	11.32 (1.60)	8.60 (2.89)	9.30 (2.59)	5.75 (1.75)
Tillers (#)	13.80 (2.21)	40.56 (6.39)	20.78 (4.56)	26.63 (4.92)	11.44 (2.01)
Height (mm)	490.00 (31.55)	417.78 (15.61)	403.33 (16.67)	540.00 (41.58)	543.33 (58.40)
Basal area (mm^2)	4950 (1189)	7367 (1581)	11,556 (3040)	11,200 (2859)	4767 (1816)
Seed heads (#)	0.50 (0.22)	2.33 (1.31)	0.78 (0.46)	5.13 (1.41)	0.11 (0.11)
RCD (mm)	1.77 (0.13)	0.94 (0.15)	1.52 (0.07)	1.29 (0.12)	1.59 (0.13)

indicative of a moderately conservative stomatal strategy—a slope of 1 would indicate a completely anisohydric species with very little regulation of leaf water status as soil moisture declines (Martínez-Vilalta et al., 2014). This varied by ecotype however, with individual slope coefficients ranging from 0.32 to 0.97 (Table 2; Figure S2). Notably, many species (9 of 11 ecotypes) experienced TLP prior to $P50_{gs}$ (Figure S3), and no correlation between TLP and P50gs was observed (Figure S4), suggesting TLP may not be a good proxy for stomatal closure for these species. However, the 95% confidence intervals for TLP and $P50_{gs}$ overlap for five of the 11 ecotypes, three of which experienced TLP prior to $P50_{gs}$ (Figure S3; Table 2).

We observed strong coordination of hydraulic and stomatal traits across grass ecotypes (Figure 3; Figure S4). Ecotypes with more negative TLP also experienced loss of K_{leaf} at more negative Ψ_{leaf} ($r = 0.69$ and 0.72 for the relationship between TLP and $P50_{Kleaf}$ and $P88_{Kleaf}$, respectively). Additionally, $P50_{gs}$ was positively correlated with $P50_{Kleaf}$ ($r = 0.6$), but not $P88_{Kleaf}$ (Figure 3). The Ψ_{leaf} slope coefficients were positively correlated with TLP ($r = 0.829$), $P50_{gs}$ ($r = 0.69$), and $P88_{Kleaf}$ ($r = 0.60$). Species with more negative $P88_{Kleaf}$ tended to have higher LDMC ($r = −0.694$). Finally, the leaf modulus of elasticity (ε) was negatively correlated with several hydraulic traits, namely TLP ($r = −0.749$), $P50_{gs}$ ($r = −0.697$), and $P50_{Kleaf}$ ($r = −0.724$), but positively correlated with LDMC ($r = 0.622$; Figure S4).

We measured several morphological traits at the end of the study on mature individuals and similarly assessed coordination across these traits using Pearson's r correlation. We observed strong positive relationships between aboveground plant biomass and several morphological traits including plant height ($r = 0.695$), basal area ($r = 0.966$), root collar diameter ($r = 0.873$), and the number of seed heads ($r = 0.808$; Figure S4). These traits were also strongly positively correlated with each other (Figure S4). Interestingly, we observed no significant relationship between the number of tillers produced and the other morphological traits or biomass production (Figure S4).

We observed several statistically significant correlations between morphological and hydraulic traits for these grasses. Specifically, $P88_{Kleaf}$ (and sometimes $P50_{Kleaf}$) was positively correlated with traits associated with increased plant size (e.g. seed head production, root collar diameter, basal area, height, and total biomass), while LDMC was negatively correlated with these same traits (Figure S4). Morphological traits were not correlated with $P50_{gs}$, Ψ_{leaf} slope, ε, or TLP.

We observed clear trade-offs in multivariate trait space (Figure 5). For example, the first principal component (PC1), which explained ~56% of trait variation across ecotypes, revealed a potential tradeoff between hydraulic vulnerability and plant productivity. Specifically, positive scores along PC1 were associated with taller and more productive species as well as high $P88_{Kleaf}$ and $P50_{Kleaf}$ (i.e. leaf hydraulic conductance declined at less negative leaf water potentials for those species). Additionally, positive PC1 scores were associated with low LDMC. The second principal component (PC2), which explained ~22% of trait variation, was also associated with

CH ARCO	CH CECI	CH THTR	NY AUSC	NY CECI	NY CHTR
−1.28 (−1.50, −0.85)	−1.17 (−1.23, −1.13)	−1.45 (−1.57, −1.28)	−2.43 (−2.62, −1.96)	−1.15 (−1.23, −1.08)	−1.73 (−1.92, −1.48)
−2.7 (NA, −1.97)	−1.55 (−1.7, −1.45)	−2.28 (NA, −1.87)	−3.61 (NA, −3.09)	−1.52 (−1.76, −1.37)	−2.64 (−2.28, −3.78)
−1.92 (−2.11, −1.74)	−2.57 (−3.80, −2.03)	−2.62 (−3.51, −1.96)	−2.68 (−2.83, −2.47)	−1.85 (−2.4, −1.39)	−2.38 (−2.67, −2.08)
−1.52 (−1.62, −1.42)	−1.45 (−1.68, −1.22)	−1.35 (−1.59, −1.11)	−2.78 (−3.02, −2.54)	−1.66 (−1.78, −1.53)	−1.62 (−1.90, −1.34)
9.70 (1.50)	12.25 (0.65)	12.18 (1.44)	19.99 (2.13)	9.86 (1.05)	16.76 (2.44)
0.32 (0.03)	0.21 (0.002)	0.30 (0.01)	0.36 (0.02)	0.22 (0.01)	0.33 (0.02)
0.81 [7]	0.78 [6]	0.92 [10]	0.65 [3]	0.86 [8]	0.89 [9]
11.39 (2.07)	50.31 (2.65)	5.25 (1.11)	8.32 (1.14)	37.70 (4.13)	17.88 (3.11)
23.00 (5.84)	33.50 (3.08)	22.67 (11.67)	35.10 (3.76)	27.60 (3.10)	39.80 (6.39)
515.56 (38.30)	648.00 (23.98)	463.33 (35.78)	447.00 (16.20)	531.00 (23.59)	528.00 (33.79)
5422 (1267)	32,830 (2759)	4267 (1069)	8040 (1560)	24,700 (2328)	14,430 (2864)
10.11 (1.35)	16.40 (1.86)	3.56 (0.65)	1.70 (0.62)	14.80 (2.35)	2.40 (0.50)
1.25 (0.10)	2.34 (0.14)	1.26 (0.14)	1.16 (0.14)	2.52 (0.16)	1.34 (0.13)
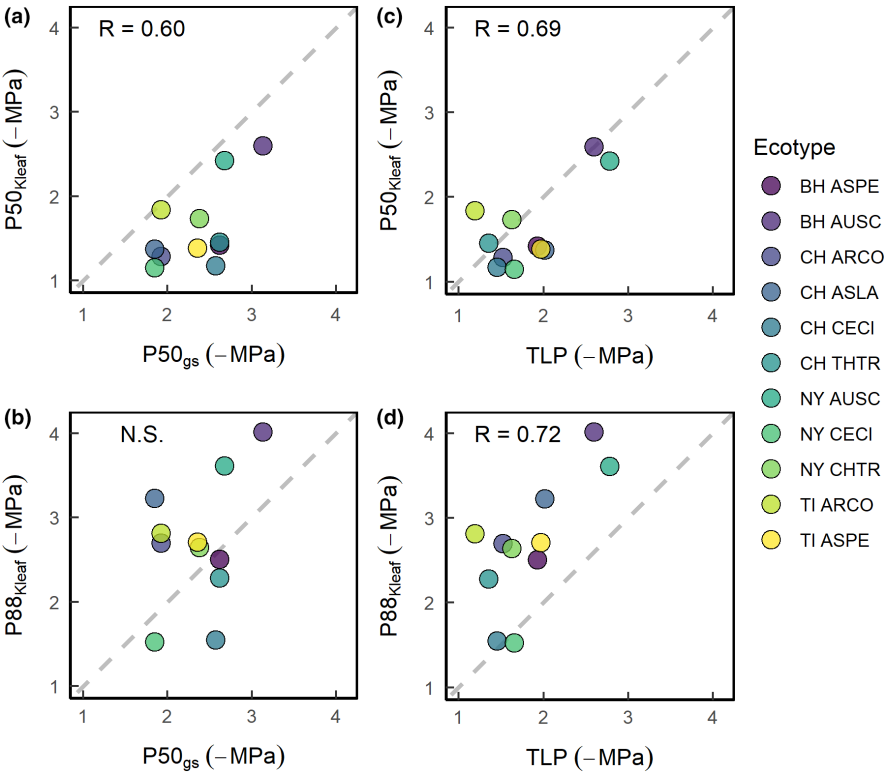
FIGURE 3 Relationships between key hydraulic and stomatal thresholds including the Ψ_{leaf} at 50% loss of stomatal conductance ($P50_{gs}$) (a and b), 50% loss of hydraulic conductance ($P50_{Kleaf}$) (a and c), 88% loss of hydraulic conductance ($P88_{Kleaf}$) (b and d), and leaf turgor loss point (TLP) (c and d). The 1:1 line is represented by a dotted grey line to indicate the timing of key thresholds (i.e. all ecotypes reach $P50_{Kleaf}$ prior to $P50_{gs}$ in panel (a). The Pearson R correlation showing strength of the relationship between two traits is shown in the top left corner of each panel unless the correlation was not statistically significant (N.S.) at $\alpha = 0.05$.

trade-offs between productivity and drought tolerance. In this case, positive PC2 scores were associated with greater tiller production, basal area, and overall biomass yet low (more negative) $P50_{gs}$.

Finally, we extracted the species scores along both PC1 and PC2 and found that variation in scores was not related to MAP, AI, or precipitation variability (Table 3). Additionally, we did not observe

significant bi-variate relationships between traits and climate of origin (Table S1).

4 | DISCUSSION

We characterized the hydraulic and stomatal strategies of several Australian grasses. Overall, more than half of the grass ecotypes experienced partial stomatal closure (P50$_{gs}$) before 88% loss of K$_{leaf}$ occurred (Table 2). This suggests the stomatal behaviour of most of the ecotypes fits the drought avoidance strategy, although there is evidence that a drought resistance strategy may also be present among some dominant Australian grasses. The prevalence of a drought avoidance strategy among grasses confirms findings for grasses in the northern hemisphere (Ocheltree et al., 2016); however, it is surprising given the growth habit of many of these species. Whereas woody species avoid loss of K$_{leaf}$ due to potentially lethal consequences (Brodribb et al., 2020), grasses frequently senesce leaves to prevent water loss only to re-sprout when soil moisture returns (Volaire & Norton, 2006). This strategy is particularly common in pulse-driven ecosystems, where a "boom or bust" strategy is more adaptive than traditional dehydration tolerance mechanisms (Schwinning & Ehleringer, 2001). Indeed, some of the perennial grasses studied here, such as *Astrebla lappacea*, can go dormant for several decades during drought (Cunningham & Leigh, 2011). Given the ubiquity of this re-sprouting strategy among grasses, it is

counterintuitive that grasses would invest in drought tolerant xylem to avoid loss in K$_{leaf}$. Nonetheless, our data, as well as recent findings from Australian pasture grasses (Jacob et al., 2022), support the conclusion that grasses invest in drought resistant xylem. Interestingly, many of the species studied here lost turgor prior to 50% loss of g$_s$. Although TLP is predicted to occur prior to stomatal closure, the opposite response is not unheard of (Bartlett et al., 2016; Farrell et al., 2017). Thus, TLP may not be a good proxy for stomatal closure as has been suggested (Meinzer et al., 2016), at least for grasses.

Previous studies have simultaneously tracked declines in K$_{leaf}$ and g$_s$ during drought to identify hydraulic safety margins with the assumption that reduced K$_{leaf}$ reflects xylem cavitation (Skelton et al., 2015); however, the rehydration kinetics method used here to quantify P88$_{Kleaf}$ and P50$_{Kleaf}$ does not directly measure cavitation events (Brodribb & Holbrook, 2003). Indeed, recent analyses of monocot responses to drought indicated that significant declines in K$_{leaf}$ can occur prior to a visual detection of cavitation events in the leaf (Jacob et al., 2022; Ocheltree et al., 2020). Thus, declines in K$_{leaf}$ during dehydration observed here are likely due to resistance in the extra-xylary pathway of water transport unrelated to cavitation, such as membrane damage and leakage (Ocheltree et al., 2020). The strong negative relationship between P50$_{Kleaf}$ and the leaf modulus of elasticity (ε) supports this conclusion (Figure S4). Species with high ε generally have rigid cells that retain water and prevent cell shrinkage (Bartlett et al., 2012). Here, species with rigid cell walls (high ε) were able to maintain K$_{leaf}$ at more negative Ψ$_{leaf}$ (low P50$_{Kleaf}$). Thus, disruptions to the cellular integrity of species with elastic cell walls (low ε) may have led to more rapid declines in K$_{leaf}$ during dehydration. We also found that species with low ε lost turgor at relatively high Ψ$_{leaf}$ (Figure S4). Compared to species with rigid cell walls, grasses with low ε have a greater capacity to lower TLP as Ψ$_{leaf}$ declines (Knapp, 1984); however, there is no direct mechanistic link between ε and TLP (Bartlett et al., 2012). Rather, high ε and thus reduced water loss can compensate for shifts in osmotic potential (i.e. the main driver of TLP) in order to maintain sufficient leaf relative water content (Bartlett et al., 2012). Therefore, this correlation likely reflects the need for low TLP species to maintain sufficient relative water content as Ψ$_{leaf}$ declines.

Overall, we found support for our hypothesis that hydraulic traits would be coordinated across the conservative-acquisitive spectrum (Reich, 2014). More drought tolerant species that experienced declines in K$_{leaf}$ at more negative Ψ$_{leaf}$ also had more negative TLP and P50$_{gs}$ and higher LDMC (Figure S4). Surprisingly, we did not observe a strong correlation between TLP and LDMC (Figure S4) as was observed across 28 European graminoid species (Májeková et al., 2021). This may reflect the low phylogenetic breadth of our study compared to Májeková et al. (2021) or perhaps different drivers of variation in LDMC across species (i.e. structural vs. non-structural carbohydrates). The positive correlation between hydraulic traits and the Ψ$_{leaf}$ slope coefficients suggests drought tolerant grasses also have tighter control of their leaf hydration status (low Ψ$_{leaf}$ slope; isohydric strategy) than less drought tolerant species. In other words, species that are capable of maintaining turgor and
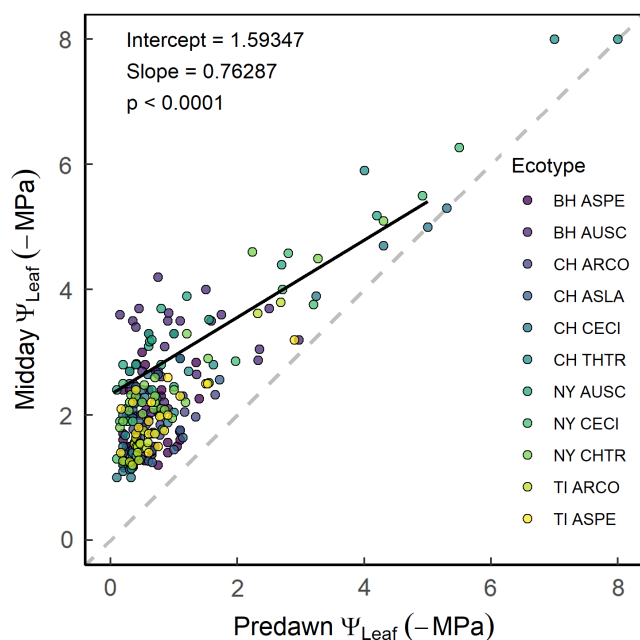
FIGURE 4 Pre-dawn versus mid-day leaf water potential. The black line represents the full model across all species. The 1:1 line is represented by a dotted grey line. According to Meinzer et al. (2016), an acquisitive perfectly anisohydric species would have a slope of 1, while a conservative or perfectly isohydric species would have a slope of 0. See Table 1 for species and site abbreviations. See Figure S2 for individual relationships.
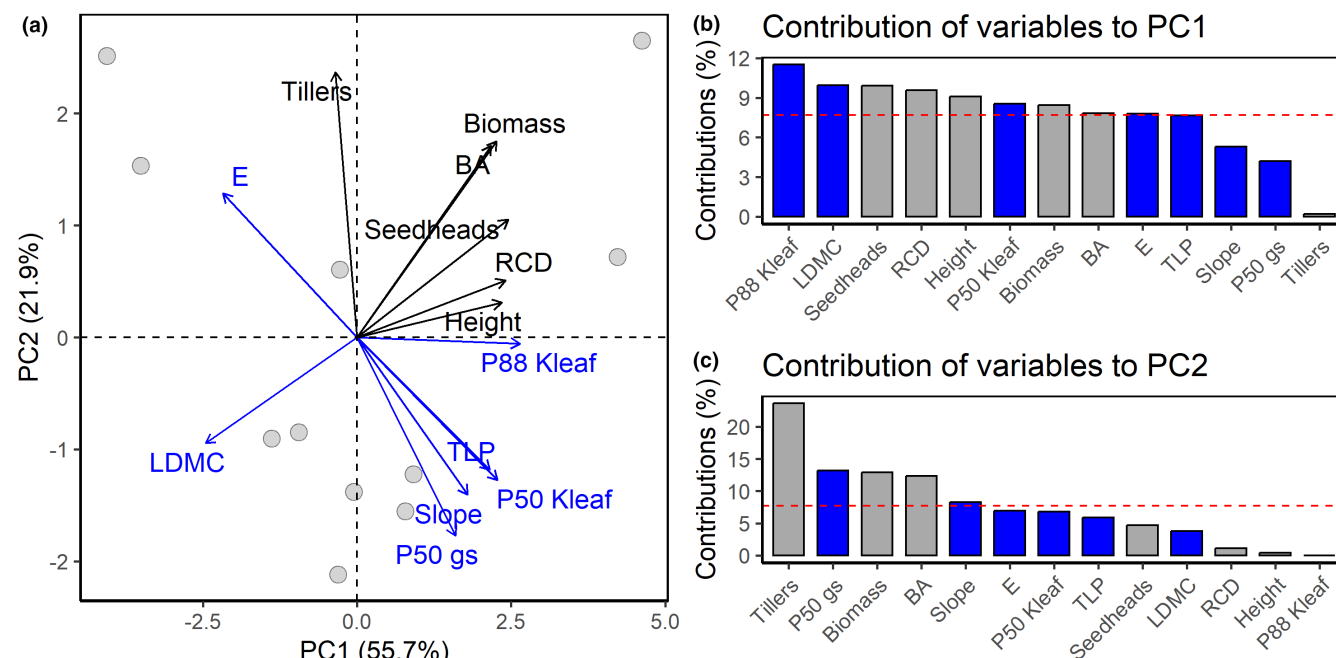
FIGURE 5 Biplot of the 1st and 2nd principal components from a principal component analysis including all hydraulic and morphological traits (a). Species/ecotypes are shown as grey circles. The arrows indicate the direction and strength of the association of hydraulic (blue) and morphological (black) traits with each axis. The 1st principal component (PC1) explained 55.7% of trait variation and was primarily associated with leaf hydraulic conductance (i.e. $P88_{Kleaf}$ and $P50_{Kleaf}$), leaf dry matter content (LDMC), and productivity (i.e. RCD, seedheads, height, and height) (b). The 2nd principal component (PC2) explained 21.9% of trait variation and was primarily assocaited with tiller production, stomatal conductance (i.e. $P50_{gs}$ and Ψ_{leaf} slope), and productivity (e.g. biomass and basal area) (c). The reference line in panels (b and c) denote the % contribution if all tratis contributed equally. See Table 2 for other trait abbreviations.

TABLE 3 Type II MANOVA (Pillai test statistic) to test for significant effects of climate of origin on individual scores along PC1 and PC2.

Coefficient	Test statistic	*p*-value
MAP	0.0402	0.8843
MAP CV	0.1211	0.6790
AI	0.0116	0.9657

Abbreviations: AI, Aridity index; MAP, mean annual precipitation; MAP CV, interannual coefficient of variation in precipitation.

K_{leaf} despite significant dehydration also have mechanisms to avoid such dehydration. By that same logic, less drought tolerant species operate at the margin of stomatal safety, which may reflect the traditional "boom or bust" strategy of arid land ecosystems (Schwinning & Ehleringer, 2001). The positive correlation between Ψ_{leaf} slope and $P50_{gs}$ suggests species that close stomata at more negative Ψ_{leaf} (low $P50_{gs}$) also have tight control of leaf water status (lower slope) and perhaps operate at a lower Ψ_{leaf} under optimal conditions due to high transpiration rates (Martínez-Vilalta et al., 2014). The method of Martínez-Vilalta et al. (2014) assumes Ψ_{leaf} equilibrates with soil moisture at night. However, species and populations can vary significantly in their rates of nocturnal stomatal conductance and/or transpiration (Chieppa, Brown, et al., 2020; Resco de Dios et al., 2019) which can be 40%–75% of daytime rates in arid environments (Ogle et al., 2012) and can lead to Ψ_{leaf} disequilibrium with

the soil (Donovan et al., 2001). While we did not measure stomatal conductance at night, this phenomenon may contribute to the more negative pre-dawn Ψ_{leaf} for some ecotypes as C_4 grasses generally have higher relative rates of nocturnal stomatal conductance compared to trees and forbs (O'Keefe & Nippert, 2018; Resco de Dios et al., 2019; Yu et al., 2019).

We found strong support for our second hypothesis that hydraulic traits would be correlated with plant size (Figure 5). Specifically, taller more productive species had less drought tolerant leaves that lost K_{leaf} at less negative Ψ_{leaf}. This follows patterns observed in woody species (McGregor et al., 2021) and is consistent with a safety vs efficiency tradeoff whereby investing in acquisitive resource use strategies (high biomass production) comes at a cost of stress tolerance (Grime 1977). Larger grass species may also have deeper roots (Schenk & Jackson, 2002), in which case increased access to deeper soil moisture reduces the need to invest in drought tolerant leaves. However, our measurements were conducted on potted plants which had the same rooting volume. Morphological traits were also strongly correlated with biomass (Figure S4), which could improve allometric estimates of productivity in the field (Chieppa, Power, et al., 2020). Interestingly, tiller density was the only morphological trait not significantly correlated with biomass. Of all traits, tiller density contributed most to the second principal component (Figure 5c), which was also strongly associated with hydraulic traits, whereby species with high tiller density had low TLP and $P50_{gs}$. Together, this suggests two primary morphological-hydraulic strategies exist for these perennial

grasses—(1) grow tall and produce more biomass or (2) produce many tillers. Strategy (1) comes at a cost of low drought tolerance, particularly related to K_{leaf}. Strategy (2) is associated with high drought tolerance and maintained stomatal conductance as Ψ_{leaf} declines. It makes sense for species capable of producing many tillers to maintain g_s given that additional tillers can be produced if senescence occurs.

Contrary to our hypothesis, we found no correlation between climate of origin and hydraulic or morphological traits. However, trait-climate relationships are often masked by the coexistence of species with divergent traits, meaning such patterns may emerge if traits were weighted by relative abundance at the community level (Griffin-Nolan et al., 2018). While the same unweighted traits have been linked to climate of origin in other grassland communities (Griffin-Nolan, Ocheltree, et al., 2019; Ocheltree et al., 2016), the environmental gradient surveyed here may not have been broad enough to capture these trends. Alternatively, this may reflect the pulse-driven nature of the ecosystems these species inhabit, where belowground traits determine re-sprouting potential and fitness. Climate may therefore be a stronger driver of belowground carbon storage traits (e.g. bud bank density) than drought tolerance traits in these ecosystems.

5 | CONCLUSIONS

Perennial grasses are an invaluable and often underappreciated plant functional group providing forage material for grazers while also capturing and storing significant carbon belowground (Pendall et al., 2018). Rangeland grasses are increasingly at risk from rising global temperatures and increased drought severity (Knapp et al., 2015; Trenberth et al., 2014), especially in Australia (Delworth & Zeng, 2014; Evans et al., 2017). We characterized the leaf hydraulic and stomatal strategies of several eastern Australian rangeland grasses and found them to be variable but largely conservative (50% stomatal closure occurs and leaves lose turgor prior to significant loss of K_{leaf}), which is similar to findings for woody plants (Creek et al., 2020; Martin-StPaul et al., 2017) and recent work on pasture grasses (Jacob et al., 2022). Certain species operate near this threshold, exhibiting a "boom or bust" strategy characteristic of dryland plant communities. We observed trade-offs between morphology and leaf water-use strategies, whereby tall productive grass species had drought intolerant leaves, while species with greater tiller density had drought tolerant leaves. Overall, the trade-off related to height and drought tolerance was similar to what has been observed in woody plants (McGregor et al., 2021), whereas the tradeoff between stomatal strategies and tiller production is unique to grasses and warrants further investigation. Although we did not find broad trait-climate relationships, these trait syndromes are likely informative of species-specific responses to drought and rainfall variability.

AUTHOR CONTRIBUTIONS

All authors contributed to the design of the experiment; Robert J. Griffin-Nolan and Jeff Chieppa collected the data; Robert J. Griffin-Nolan analysed the data and wrote the initial draft of the manuscript with comments from all authors.

CONFLICT OF INTEREST STATEMENT

None of the authors have a conflict of interest.

DATA AVAILABILITY STATEMENT

Data available from the Dryad Digital Repository: https://doi.org/10.5061/dryad.jsxksn0f8 (Griffin-Nolan et al., 2023).

ORCID

Robert J. Griffin-Nolan https://orcid.org/0000-0002-9411-3588
Jeff Chieppa https://orcid.org/0000-0003-2854-1514
Alan K. Knapp https://orcid.org/0000-0003-1695-4696
Uffe N. Nielsen https://orcid.org/0000-0003-2400-7453
David T. Tissue https://orcid.org/0000-0002-8497-2047

REFERENCES

Anderegg, W. R. (2015). Spatial and temporal variation in plant hydraulic traits and their relevance for climate change impacts on vegetation. *New Phytologist*, *205*(3), 1008–1014. https://doi.org/10.1111/nph.12907

Bartlett, M. K., Klein, T., Jansen, S., Choat, B., & Sack, L. (2016). The correlations and sequence of plant stomatal, hydraulic, and wilting responses to drought. *Proceedings of the National Academy of Sciences of the United States of America*, *113*(46), 13098–13103. https://doi.org/10.1073/pnas.1604088113

Bartlett, M. K., Scoffoni, C., & Sack, L. (2012). The determinants of leaf turgor loss point and prediction of drought tolerance of species and biomes: A global meta-analysis. *Ecology Letters*, *15*(5), 393–405. https://doi.org/10.1111/j.1461-0248.2012.01751.x

Benito Garzón, M., Robson, T. M., & Hampe, A. (2019). ΔTrait SDMs: Species distribution models that account for local adaptation and phenotypic plasticity. *New Phytologist*, *222*(4), 1757–1765. https://doi.org/10.1111/nph.15716

Blackman, C. J., Brodribb, T. J., & Jordan, G. J. (2010). Leaf hydraulic vulnerability is related to conduit dimensions and drought resistance across a diverse range of woody angiosperms. *New Phytologist*, *188*(4), 1113–1123. https://doi.org/10.1111/j.1469-8137.2010.03439.x

Brodribb, T. J., Bienaimé, D., & Marmottant, P. (2016). Revealing catastrophic failure of leaf networks under stress. *Proceedings of the National Academy of Sciences of the United States of America*, *113*(17), 4865–4869. https://doi.org/10.1073/pnas.1522569113

Brodribb, T. J., & Holbrook, N. M. (2003). Stomatal closure during leaf dehydration, correlation with other leaf physiological traits. *Plant Physiology*, *132*(4), 2166–2173. https://doi.org/10.1104/pp.103.023879

Brodribb, T. J., Powers, J., Cochard, H., & Choat, B. (2020). Hanging by a thread? Forests and drought. *Science*, *368*(6488), 261–266. https://doi.org/10.1126/science.aat7631

Chieppa, J., Brown, T., Giresi, P., Juenger, T. E., Resco de Dios, V., Tissue, D. T., & Aspinwall, M. J. (2020). Climate and stomatal traits drive covariation in night-time stomatal conductance and day-time gas exchange rates in a widespread C4 grass. *New Phytologist*, *229*, 2020–2034. https://doi.org/10.1111/nph.16987

Chieppa, J., Power, S. A., Tissue, D. T., & Nielsen, U. N. (2020). Allometric estimates of aboveground biomass using cover and height are improved by increasing specificity of plant functional groups in eastern Australian rangelands. *Rangeland Ecology & Management*, *73*(3), 375–383. https://doi.org/10.1016/j.rama.2020.01.009

Creek, D., Lamarque, L. J., Torres-Ruiz, J. M., Parise, C., Burlett, R., Tissue, D. T., & Delzon, S. (2020). Xylem embolism in leaves does not occur with open stomata: Evidence from direct observations using the optical visualization technique. *Journal of Experimental Botany*, *71*(3), 1151–1159. https://doi.org/10.1093/jxb/erz474

Cunningham, G. M., & Leigh, J. H. (2011). *Plants of western new South Wales*. CSIRO Publishing.

De Kauwe, M. G., Medlyn, B. E., Ukkola, A. M., Mu, M., Sabot, M. E., Pitman, A. J., Meir, P., Cernusak, L. A., Rifai, S. W., Choat, B., Tissue, D. T., Blackman, C. J., Li, X., Roderick, M., & Briggs, P. R. (2020). Identifying areas at risk of drought-induced tree mortality across south-eastern Australia. *Global Change Biology*, *26*(10), 5716–5733. https://doi.org/10.1111/gcb.15215

Delworth, T. L., & Zeng, F. (2014). Regional rainfall decline in Australia attributed to anthropogenic greenhouse gases and ozone levels. *Nature Geoscience*, *7*(8), 583–587. https://doi.org/10.1038/ngeo2201

Deveautour, C., Chieppa, J., Nielsen, U. N., Boer, M. M., Mitchell, C., Horn, S., Power, S. A., Guillen, A., Bennett, A. E., & Powell, J. R. (2020). Biogeography of arbuscular mycorrhizal fungal spore traits along an aridity gradient, and responses to experimental rainfall manipulation. *Fungal Ecology*, *46*, 100899. https://doi.org/10.1016/j.funeco.2019.100899

Díaz, S., Kattge, J., Cornelissen, J. H., Wright, I. J., Lavorel, S., Dray, S., Reu, B., Kleyer, M., Wirth, C., Prentice, I. C., Garnier, E., Bönisch, G., Westoby, M., Poorter, H., Reich, P. B., Moles, A. T., Dickie, J., Gillison, A. N., Zanne, A. E., … Gorné, L. D. (2016). The global spectrum of plant form and function. *Nature*, *529*(7585), 167–171. https://doi.org/10.1038/nature16489

Donovan, L., Linton, M., & Richards, J. (2001). Predawn plant water potential does not necessarily equilibrate with soil water potential under well-watered conditions. *Oecologia*, *129*(3), 328–335. https://doi.org/10.1007/s004420100738

Duursma, R. A., & Choat, B. (2017). fitplc: An R package to fit hydraulic vulnerability curves. *Journal of Plant Hydraulics*, *4*, e002. https://doi.org/10.20870/jph.2017.e002

Evans, J. P., Argueso, D., Olson, R., & Di Luca, A. (2017). Bias-corrected regional climate projections of extreme rainfall in south-East Australia. *Theoretical and Applied Climatology*, *130*(3), 1085–1098. https://doi.org/10.1007/s00704-016-1949-9

Farrell, C., Szota, C., & Arndt, S. K. (2017). Does the turgor loss point characterize drought response in dryland plants? *Plant, Cell & Environment*, *40*(8), 1500–1511. https://doi.org/10.1111/pce.12948

Funk, J. L., Larson, J. E., Ames, G. M., Butterfield, B. J., Cavender-Bares, J., Firn, J., Laughlin, D. C., Sutton-Grier, A. E., Williams, L., & Wright, J. (2017). Revisiting the holy grail: Using plant functional traits to understand ecological processes. *Biological Reviews*, *92*(2), 1156–1173. https://doi.org/10.1111/brv.12275

Griffin-Nolan, R. J., Blumenthal, D. M., Collins, S. L., Farkas, T. E., Hoffman, A. M., Mueller, K. E., Ocheltree, T. W., Smith, M. D., Whitney, K. D., & Knapp, A. K. (2019). Shifts in plant functional composition following long-term drought in grasslands. *Journal of Ecology*, *107*(5), 2133–2148. https://doi.org/10.1111/1365-2745.13252

Griffin-Nolan, R. J., Bushey, J. A., Carroll, C. J., Challis, A., Chieppa, J., Garbowski, M., Hoffman, A. M., Post, A. K., Slette, I. J., Spitzer, D., Zambonini, D., Ocheltree, T. W., Tissue, D. T., & Knapp, A. K. (2018). Trait selection and community weighting are key to understanding ecosystem responses to changing precipitation regimes. *Functional Ecology*, *32*(7), 1746–1756. https://doi.org/10.1111/1365-2435.13135

Griffin-Nolan, R. J., Ocheltree, T. W., Mueller, K. E., Blumenthal, D. M., Kray, J. A., & Knapp, A. K. (2019). Extending the osmometer method for assessing drought tolerance in herbaceous species. *Oecologia*, *189*(2), 353–363. https://doi.org/10.1007/s00442-019-04336-w

Griffin-Nolan, R., Chieppa, J., Knapp, A. K., Nielsen, U. N., & Tissue, D. T. (2023). Coordination of hydraulic and morphological traits across dominant grasses in eastern Australia. *Dryad Dataset*. https://doi.org/10.5061/dryad.jsxksn0f8

Holloway-Phillips, M. M., & Brodribb, T. J. (2011). Minimum hydraulic safety leads to maximum water-use efficiency in a forage grass. *Plant, Cell & Environment*, *34*(2), 302–313. https://doi.org/10.1111/j.1365-3040.2010.02244.x

Hoover, D. L., Koriakin, K., Albrigtsen, J., & Ocheltree, T. (2019). Comparing water-related plant functional traits among dominant grasses of the Colorado plateau: Implications for drought resistance. *Plant and Soil*, *441*(1), 207–218. https://doi.org/10.1007/s11104-019-04107-9

Jacob, V., Choat, B., Churchill, A. C., Zhang, H., Barton, C. V., Krishnananthaselvan, A., Post, A. K., Power, S. A., Medlyn, B. E., & Tissue, D. T. (2022). High safety margins to drought-induced hydraulic failure found in five pasture grasses. *Plant, Cell & Environment*, *45*, 1631–1646. https://doi.org/10.1111/pce.14318

Jardine, E. C., Thomas, G. H., & Osborne, C. P. (2021). Traits explain sorting of C4 grasses along a global precipitation gradient. *Ecology and Evolution*, *11*(6), 2669–2680. https://doi.org/10.1002/ece3.7223

Knapp, A. K. (1984). Water relations and growth of three grasses during wet and drought years in a tallgrass prairie. *Oecologia*, *65*(1), 35–43. https://doi.org/10.1007/BF00384460

Knapp, A. K., Carroll, C. J. W., Denton, E. M., La Pierre, K. J., Collins, S. L., & Smith, M. D. (2015). Differential sensitivity to regional-scale drought in six central US grasslands. *Oecologia*, *177*(4), 949–957. https://doi.org/10.1007/s00442-015-3233-6

Koide, R. T., Robichaux, R. H., Morse, S. R., & Smith, C. M. (1989). Plant water status, hydraulic resistance and capacitance. In *Plant physiological ecology* (pp. 161–183). Springer.

Konings, A. G., & Gentine, P. (2017). Global variations in ecosystem-scale isohydricity. *Global Change Biology*, *23*(2), 891–905. https://doi.org/10.1111/gcb.13389

Laliberté, E., & Legendre, P. (2010). A distance-based framework for measuring functional diversity from multiple traits. *Ecology*, *91*(1), 299–305. https://doi.org/10.1890/08-2244.1

Lens, F., Picon-Cochard, C., Delmas, C. E., Signarbieux, C., Buttler, A., Cochard, H., Jansen, S., Chauvin, T., Doria, L. C., Del Arco, M., & Delzon, S. (2016). Herbaceous angiosperms are not more vulnerable to drought-induced embolism than angiosperm trees. *Plant Physiology*, *172*(2), 661–667. https://doi.org/10.1104/pp.16.00829

Májeková, M., Hájek, T., Albert, Á. J., de Bello, F., Doležal, J., Götzenberger, L., Janeček, S., Lepš, J., Liancourt, P., & Mudrák, O. (2021). Weak coordination between leaf drought tolerance and proxy traits in herbaceous plants. *Functional Ecology*, *35*(6), 1299–1311. https://doi.org/10.1111/1365-2435.13792

Martínez-Vilalta, J., & Garcia-Forner, N. (2017). Water potential regulation, stomatal behaviour and hydraulic transport under

drought: Deconstructing the iso/anisohydric concept. *Plant, Cell & Environment*, 40(6), 962–976. https://doi.org/10.1111/pce.12846

Martínez-Vilalta, J., Poyatos, R., Aguadé, D., Retana, J., & Mencuccini, M. (2014). A new look at water transport regulation in plants. *New Phytologist*, 204(1), 105–115. https://doi.org/10.1111/nph.12912

Martin-StPaul, N., Delzon, S., & Cochard, H. (2017). Plant resistance to drought depends on timely stomatal closure. *Ecology Letters*, 20(11), 1437–1447. https://doi.org/10.1111/ele.12851

McDowell, N., Pockman, W. T., Allen, C. D., Breshears, D. D., Cobb, N., Kolb, T., Plaut, J., Sperry, J., West, A., Williams, D. G., & Yepez, E. A. (2008). Mechanisms of plant survival and mortality during drought: Why do some plants survive while others succumb to drought? *New Phytologist*, 178(4), 719–739. https://doi.org/10.1111/j.1469-8137.2008.02436.x

McGregor, I. R., Helcoski, R., Kunert, N., Tepley, A. J., Gonzalez-Akre, E. B., Herrmann, V., Zailaa, J., Stovall, A. E. L., Bourg, N. A., McShea, W. J., Pederson, N., Sack, L., & Anderson-Teixeira, K. J. (2021). Tree height and leaf drought tolerance traits shape growth responses across droughts in a temperate broadleaf forest. *New Phytologist*, 231(2), 601–616. https://doi.org/10.1111/nph.16996

Meinzer, F. C., Woodruff, D. R., Marias, D. E., Smith, D. D., McCulloh, K. A., Howard, A. R., & Magedman, A. L. (2016). Mapping 'hydroscapes' along the iso- to anisohydric continuum of stomatal regulation of plant water status. *Ecology Letters*, 19, 1343–1352. https://doi.org/10.1111/ele.12670

Ocheltree, T., Gleason, S., Cao, K.-F., & Jiang, G.-F. (2020). Loss and recovery of leaf hydraulic conductance: Root pressure, embolism, and extra-xylary resistance. *Journal of Plant Hydraulics*, 7, e–001. https://doi.org/10.20870/jph.2020.e-001

Ocheltree, T. W., Nippert, J. B., & Prasad, P. V. (2016). A safety vs efficiency trade-off identified in the hydraulic pathway of grass leaves is decoupled from photosynthesis, stomatal conductance and precipitation. *New Phytologist*, 210(1), 97–107. https://doi.org/10.1111/nph.13781

Ogle, K., Lucas, R. W., Bentley, L. P., Cable, J. M., Barron-Gafford, G. A., Griffith, A., Ignace, D., Jenerette, G. D., Tyler, A., Huxman, T. E., Loik, M. E., Smith, S. D., & Tissue, D. T. (2012). Differential daytime and night-time stomatal behavior in plants from north American deserts. *New Phytologist*, 194(2), 464–476. https://doi.org/10.1111/j.1469-8137.2012.04068.x

O'Keefe, K., & Nippert, J. B. (2018). Drivers of nocturnal water flux in a tallgrass prairie. *Functional Ecology*, 32(5), 1155–1167. https://doi.org/10.1111/1365-2435.13072

Pendall, E., Bachelet, D., Conant, R. T., El Masri, B., Flanagan, L. B., Knapp, A. K., Liu, J., Liu, S., & Schaeffer, S. M. (2018). Chapter 10: Grasslands. In N. Cavallaro, G. Shrestha, R. Birdsey, M. A. Mayes, R. G. Najjar, S. C. Reed, P. Romero-Lankao, & Z. Zhu (Eds.), *Second state of the carbon cycle report (SOCCR2): A sustained assessment report* (pp. 399–427). U.S. Global Change Research Program.

Perez-Harguindeguy, N., Diaz, S., Garnier, E., Lavorel, S., Poorter, H., Jaureguiberry, P., Bret-Harte, M. S., Cornwell, W. K., Craine, J. M., Gurvich, D. E., Urcelay, C., Veneklaas, E. J., Reich, P. B., Poorter, L., Wright, I. J., Ray, P., Enrico, L., Pausas, J. G., de Vos, A. C., … Cornelissen, J. H. C. (2016). Corrigendum to: New handbook for standardised measurement of plant functional traits worldwide. *Australian Journal of Botany*, 64(8), 715–716. https://doi.org/10.1071/BT12225_CO

Reich, P. B. (2014). The world-wide 'fast–slow' plant economics spectrum: A traits manifesto. *Journal of Ecology*, 102(2), 275–301. https://doi.org/10.1111/1365-2745.12211

Resco de Dios, V., Chowdhury, F. I., Granda, E., Yao, Y., & Tissue, D. T. (2019). Assessing the potential functions of nocturnal stomatal conductance in C3 and C4 plants. *New Phytologist*, 223, 1696–1706. https://doi.org/10.1111/nph.15881

Ritchie, G. A., & Hinckley, T. M. (1975). The pressure chamber as an instrument for ecological research. *Advances in Ecological Research*, 9, 165–254. https://doi.org/10.1016/S0065-2504(08)60290-1

Rosado, B. H., Dias, A. T., & de Mattos, E. A. (2013). Going back to basics: Importance of ecophysiology when choosing functional traits for studying communities and ecosystems. *Natureza & Conservação*, 11(1), 15–22. https://doi.org/10.4322/natcon.2013.002

Sack, L., Cowan, P. D., Jaikumar, N., & Holbrook, N. M. (2003). The 'hydrology' of leaves: co-ordination of structure and function in temperate woody species. *Plant, Cell & Environment*, 26(8), 1343–1356. https://doi.org/10.1046/j.0016-8025.2003.01058.x

Sandel, B., Monnet, A. C., & Vorontsova, M. (2016). Multidimensional structure of grass functional traits among species and assemblages. *Journal of Vegetation Science*, 27(5), 1047–1060. https://doi.org/10.1111/jvs.12422

Schenk, H. J., & Jackson, R. B. (2002). Rooting depths, lateral root spreads and below-ground/above-ground allometries of plants in water-limited ecosystems. *Journal of Ecology*, 90, 480–494. https://doi.org/10.1046/j.1365-2745.2002.00682.x

Schulte, P. J., & Hinckley, T. M. (1985). A comparison of pressure-volume curve data analysis techniques. *Journal of Experimental Botany*, 36(10), 1590–1602. https://doi.org/10.1093/jxb/36.10.1590

Schwinning, S., & Ehleringer, J. R. (2001). Water use trade-offs and optimal adaptations to pulse-driven arid ecosystems. *Journal of Ecology*, 89(3), 464–480. https://doi.org/10.1046/j.1365-2745.2001.00576.x

Scoffoni, C., Rawls, M., McKown, A., Cochard, H., & Sack, L. (2011). Decline of leaf hydraulic conductance with dehydration: Relationship to leaf size and venation architecture. *Plant Physiology*, 156(2), 832–843. https://doi.org/10.1104/pp.111.173856

Simpson, K. J., Archibald, S., & Osborne, C. P. (2022). Savanna fire regimes depend on grass trait diversity. *Trends in Ecology & Evolution*, 37, 749–758. https://doi.org/10.1016/j.tree.2022.04.010

Skelton, R. P., West, A. G., & Dawson, T. E. (2015). Predicting plant vulnerability to drought in biodiverse regions using functional traits. *Proceedings of the National Academy of Sciences of the United States of America*, 112(18), 5744–5749. https://doi.org/10.1073/pnas.1503376112

Sonawane, B. V., Koteyeva, N. K., Johnson, D. M., & Cousins, A. B. (2021). Differences in leaf anatomy determines temperature response of leaf hydraulic and mesophyll CO2 conductance in phylogenetically related C4 and C3 grass species. *New Phytologist*, 230(5), 1802–1814. https://doi.org/10.1111/nph.17287

Suding, K. N., Lavorel, S., Chapin, F. S., Cornelissen, J. H. C., Díaz, S., Garnier, E., Goldberg, D., Hooper, D. U., Jackson, S. T., & Navas, M.-L. (2008). Scaling environmental change through the community-level: A trait-based response-and-effect framework for plants. *Global Change Biology*, 14(5), 1125–1140. Portico. https://doi.org/10.1111/j.1365-2486.2008.01557.x

Tardieu, F., & Simonneau, T. (1998). Variability among species of stomatal control under fluctuating soil water status and evaporative demand: Modelling isohydric and anisohydric behaviours. *Journal of Experimental Botany*, 49, 419–432. http://www.jstor.org/stable/23695975

Timbal, B., & Fawcett, R. (2013). A historical perspective on southeastern Australian rainfall since 1865 using the instrumental record. *Journal of Climate*, 26(4), 1112–1129. https://doi.org/10.1175/JCLI-D-12-00082.1

Trenberth, K. E., Dai, A., Van Der Schrier, G., Jones, P. D., Barichivich, J., Briffa, K. R., & Sheffield, J. (2014). Global warming and changes in drought. *Nature Climate Change*, 4(1), 17–22. https://doi.org/10.1038/nclimate2067

Turner, N. C. (1988). Measurement of plant water status by the pressure chamber technique. *Irrigation Science*, 9(4), 289–308. https://doi.org/10.1007/BF00296704

van der Plas, F., Schröder-Georgi, T., Weigelt, A., Barry, K., Meyer, S., Alzate, A., Barnard, R. L., Buchmann, N., de Kroon, H., Ebeling, A.,

Eisenhauer, N., Engels, C., Fischer, M., Gleixner, G., Hildebrandt, A., Koller-France, E., Leimer, S., Milcu, A., Mommer, L., ... Wirth, C. (2020). Plant traits alone are poor predictors of ecosystem properties and long-term ecosystem functioning. *Nature Ecology & Evolution*, *4*(12), 1602–1611. https://doi.org/10.1038/s41559-020-01316-9

Van Etten, E. J. (2009). Inter-annual rainfall variability of arid Australia: Greater than elsewhere? *Australian Geographer*, *40*(1), 109–120. https://doi.org/10.1080/00049180802657075

Vander Weide, B. L., Hartnett, D. C., & Carter, D. L. (2014). Belowground bud banks of tallgrass prairie are insensitive to multi-year, growing-season drought. *Ecosphere*, *5*(8), 1–17. https://doi.org/10.1890/ES14-00058.1

Volaire, F., & Norton, M. (2006). Summer dormancy in perennial temperate grasses. *Annals of Botany*, *98*(5), 927–933. https://doi.org/10.1093/aob/mcl195

Wilcox, K. R., Blumenthal, D. M., Kray, J. A., Mueller, K. E., Derner, J. D., Ocheltree, T., & Porensky, L. M. (2021). Plant traits related to precipitation sensitivity of species and communities in semiarid shortgrass prairie. *New Phytologist*, *229*(4), 2007–2019. https://doi.org/10.1111/nph.17000

Yu, K., Goldsmith, G. R., Wang, Y., & Anderegg, W. R. (2019). Phylogenetic and biogeographic controls of plant nighttime stomatal conductance. *New Phytologist*, *222*(4), 1778–1788. https://doi.org/10.1111/nph.15755

Zhang, C. J., Delgado-Baquerizo, M., Drake, J. E., Reich, P. B., Tjoelker, M. G., Tissue, D. T., Wang, J. T., He, J. Z., & Singh, B. K. (2018). Intraspecies variation in a widely distributed tree species regulates the responses of soil microbiome to different temperature regimes. *Environmental Microbiology Reports*, *10*(2), 167–178. https://doi.org/10.1111/1758-2229.12613

Zhou, H., Akçay, E., Edwards, E., & Helliker, B. (2020). The legacy of C4 evolution in the hydraulics of C3 and C4 grasses. *Bio Rxiv*, 2020-05. https://doi.org/10.1101/2020.05.14.097030

Zimmermann, M. H. (1983). *Xylem structure and the ascent of sap*. Springer.

SUPPORTING INFORMATION

Additional supporting information can be found online in the Supporting Information section at the end of this article.

Figure S1. Map of collection site and images of experimental set up.

Figure S2. Relationship between predawn and midday leaf water potential for each species.

Figure S3. Timing of hydraulic and stomatal thresholds.

Figure S4. Trait correlation matrix.

Figure S5. Method comparison of Martinez-Vilalta et al. (2014) versus Skelton et al. (2015).

Table S1. Pearson correlation matrix showing the correlation between climatic variables and each trait measured.